PERGAMON Computers and Mathematics with Applications 39 (2000) 81–97

An International Journal
computers & mathematics
with applications

www.elsevier.nl/locate/camwa

Heat Flows and Related Minimization Problem in Image Restoration

C. A. Z. BARCELOS*
Departamento de Matemática, Universidade Federal de Uberlândia
Uberlândia, Brazil

Y. CHEN†
Department of Mathematics, University of Florida
Gainesville, FL 32611, U.S.A.
yun@math.ufl.edu

(Received September 1998; revised and accepted June 1999)

Abstract—A new anisotropic diffusion model is proposed for image restoration and segmentation, which is closely related to the minimization problems for the unconstrained total variation $E(u) = \int_\Omega \alpha(x)|\nabla u| + (\beta/2)|u - I|^2$. Existence, uniqueness, and stability of the viscosity solutions of the equation are proved. The experimental results are given and compared with the existing models in the framework of image restoration. The improvement on preserving sharp edges by using the new model is visible.

Keywords—Image restoration, Total variation, Heat flow method, Anisotropic diffusion.

1. INTRODUCTION

In recent years, the variational method has been effectively used in the recovery of object shape from noisy images. The general approach of this method is minimizing the total variation of the image, which incorporates constraints imposed by edge detection, object matching, and other objectives. One common way to solve the minimization problem is finding the steady-state solution of a heat equation corresponding to the Euler-Lagrange equation of the total variation (energy functional). We call this method the heat flow method. In this note, we shall show that the structure of the heat equation affects the quality of the reconstructed image.

Let I be the intensity of an image obtained from a noiseless image by adding Gaussian noise with zero mean, defined on a rectangle $\Omega \subset R^2$. Also, let u represent the reconstructed image. We have $I = u + n$, where n is the noise. Our problem is to reconstruct u from I. The total variation method proposed by Rudin, Osher and Fatemi [1] consists in solving the following constrained minimization problem:

$$\text{Minimize} \int_\Omega |\nabla u|$$

$$\text{with} \int_\Omega u = \int_\Omega I \quad \text{and} \quad \int_\Omega |u - I|^2 = \eta^2.$$

*Partially supported by grants of CNPq, Brazil. This work was done while visiting the University of Florida.
†Partially supported by NSF Grant DMS 9703497.

0898-1221/00/$ - see front matter Typeset by AMS-TEX
PII: S0898-1221(00)00048-1

The first constrain indicates that the noise has zero mean, and the second one uses *a priori* information that the standard deviation of the noise $n(x)$ is η. This problem is naturally linked to the unconstrained problem

$$\text{Minimize } E(u) = \int_\Omega |\nabla u| + \frac{\beta}{2}|u - I|^2.$$

The solution was obtained by finding a steady-state solution of a time dependent partial differential equation, which is the evolution of the Euler-Lagrange equation for $E(u)$. This means that they solved

$$u_t = \operatorname{div}\left(\frac{\nabla u}{|\nabla u|}\right) - \beta(u - I), \tag{1.1}$$

$$u(x, 0) = I(x), \tag{1.2}$$

$$\left.\frac{\partial u}{\partial n}\right|_{\partial\Omega \times R_+} = 0. \tag{1.3}$$

In [2,3], a spatially adaptive total variation scheme was proposed by minimizing the functional

$$E(u) = \int_\Omega \alpha(x)|\nabla u| + \frac{\beta}{2}|u - I|^2. \tag{1.4}$$

The choice of α is dependent on the amount of detail we wish to preserve and the amount of the noise. Ideally, we wish α is a differentiable function having value zero on the edges and value one on the homogeneous regions. The Euler-Lagrange equation for (1.4) is

$$\operatorname{div}\left(\alpha(x)\left(\frac{\nabla u}{|\nabla u|}\right)\right) - \beta(u - I) = 0. \tag{1.5}$$

It was suggested in [2,4] that the minimization problem (1.4) could be solved by finding the solution of (1.5) or by finding the steady-state solution of the evolution of (1.5):

$$u_t = \operatorname{div}\left(\alpha(x)\left(\frac{\nabla u}{|\nabla u|}\right)\right) - \beta(u - I), \tag{1.6}$$

with the initial and boundary conditions (1.2) and (1.3). The numerical solution of (1.6) is readily obtained by explicit iteration scheme as opposed to implicit methods for solving a stationary equation. To solve this minimization problem, one may also consider the following heat equations rather than (1.6):

$$\begin{aligned} u_t &= |\nabla u| \operatorname{div}\left(\alpha(x)\left(\frac{\nabla u}{|\nabla u|}\right)\right) - \beta|\nabla u|(u - I) \\ &= \alpha(x)|\nabla u| \operatorname{div}\left(\frac{\nabla u}{|\nabla u|}\right) + \nabla\alpha \cdot \nabla u - \beta|\nabla u|(u - I) \end{aligned} \tag{1.7}$$

or

$$u_t = \alpha(x)\left\{\alpha(x)|\nabla u| \operatorname{div}\left(\frac{\nabla u}{|\nabla u|}\right) + \nabla\alpha \cdot \nabla u - \beta|\nabla u|(u - I)\right\}. \tag{1.7'}$$

It is a natural question which evolution equation related to the minimization problem (1.4) does a better job in image recovery. Is it the evolution of the actual Euler-Lagrange equation (1.6) or the evolution of an elliptic equation obtained by multiplying some terms to the actual Euler-Lagrange equation, such as (1.7) or (1.7')?

Comparing (1.6) with (1.7) and (1.7′), (1.7) and (1.7′) have the following advantages. First, they have a geometric interpretation. Both (1.7) and (1.7′) can be viewed as a geometry-driven diffusion scheme, where the parameter function $\alpha(x)$ controls the speed of diffusion. Let us think that the image u is formed by iso-intensity contours $u = c$. The diffusion term $\alpha(x)|\nabla u| \operatorname{div}(\nabla u/|\nabla u|)$ in (1.7) (or the diffusion term $\alpha^2(x)|\nabla u| \operatorname{div}(\nabla u/|\nabla u|)$ in (1.7′)), indicates that each iso-intensity contour moves along its normal direction with a speed $\alpha(x)k$ (or $\alpha^2 k$ for (1.7′)), where $k = \operatorname{div}(\nabla u/|\nabla u|)$ is the local curvature of the iso-intensity contour. Secondly, instead of the term $\nabla\alpha \cdot \nabla u/|\nabla u|$ in (1.6), we have the term $\nabla\alpha \cdot \nabla u$ in (1.7) (or $\alpha\nabla\alpha \cdot \nabla u$ in (1.7′)). This reduces the error in the numerical implementation caused by the presence of $|\nabla u|$ as a denominator. At last, mathematically, we are able to obtain the existence, uniqueness, and stability of the viscosity solution for (1.7) or (1.7′) with (1.2),(1.3) (we shall give the proof for the mathematical validity of (1.7′) in the Appendix), while it seems difficult to prove these for (1.6). Comparing (1.7) with (1.7′), (1.7) is the evolution of the elliptic equation obtained from (1.5) by multiplying $|\nabla u|$ and the evolution equation (1.7′) comes from (1.5) by multiplying $\alpha(x)|\nabla u|$. The major difference between these two equation is that the multiplier $|\nabla u|$ in (1.7) takes much larger value on the edges than in the homogeneous regions, while the multiplier $\alpha(x)|\nabla u|$ in (1.7′) takes smaller value on the edges than in the homogeneous regions, for a suitable choice of $\alpha(x)$. Due to this difference, (1.7) diffuses more on the edges comparing the diffusion performed by (1.6). Contrary to (1.7), the edges get less smoothing than the homogeneous regions when the diffusion is applied by (1.7′) instead of (1.6). In this note, we shall show this difference by experimental results with the choice of $\alpha(x)$ given by

$$\alpha(x) = g(\nabla G_\sigma * u) = \frac{1}{1 + K|\nabla G_\sigma * u|^2}, \tag{1.8}$$

where $G_\sigma(x) = (1/\sigma\sqrt{4\pi}) \exp(-|x|/4\sigma^2)$, $K > 0$, and $\sigma > 0$ are parameters.

With the choice of $\alpha(x)$ as in (1.8), equation (1.7) is reduced to the form

$$u_t = g(\nabla G_\sigma * u)|\nabla u| \operatorname{div}\left(\frac{\nabla u}{|\nabla u|}\right) + \nabla(g(\nabla G_\sigma * u)) \cdot \nabla u - \beta|\nabla u|(u - I). \tag{1.9}$$

This equation was studied in [5] and might be viewed as a framework for image denoising via nonlinear diffusion, and a modification of the well-known Alvarez-Lions-Morel [ALM] model:

$$u_t = g(\nabla G_\sigma * u)|\nabla u| \operatorname{div}\left(\frac{\nabla u}{|\nabla u|}\right). \tag{1.9′}$$

As analyzed in [6], in (1.9), the smoothing is made by the degenerate diffusion term $g(\nabla G_\sigma * u)|\nabla u| \operatorname{div}(\nabla u/|\nabla u|)$. This term diffuses u in the direction orthogonal to its gradient ∇u and does not diffuse at all in the direction of ∇u. Therefore, u is smoothed on both sides of an edge with a minimal smoothing of the edge itself. Moreover, the speed of the diffusion is controlled by $g(\nabla G_\sigma * u)$, so that the edges are less smoothed. However, comparing the diffusion performed by $g(\nabla G_\sigma * u) \operatorname{div}(\nabla u/|\nabla u|)$ or by $g^2(\nabla G_\sigma * u)|\nabla u| \operatorname{div}(\nabla u/|\nabla u|)$, (1.7) diffuses more on the edges than the latter two.

Similarly, the flow used in [7] for solving a minimization problem was not the evolution of the actual Euler-Lagrange equation. In [7], Shah proposed to perform simultaneous image denoising and segmentation by

$$\text{minimizing } E(u, v) = \int_\Omega \alpha(1 - v)^2|\nabla u| + \beta|u - I| + \frac{\rho}{2}|\nabla v|^2 + \frac{v^2}{2\rho}, \tag{1.10}$$

where v is considered as an edge strength function, which is smooth and takes value one on the edges and decays away from the edges to value zero in homogeneous regions. This minimization

problem was solved in [7] by solving the system

$$\partial_t u = (1-v)|\nabla u| \operatorname{div}\left(\frac{\nabla u}{|\nabla u|}\right) - 2\nabla v \cdot \nabla u - \frac{\beta}{\alpha(1-v)}|\nabla u|\frac{u-I}{|u-I|}, \tag{1.11}$$

$$\partial_t v = \Delta v - \frac{v}{\rho^2} + \frac{2\alpha}{\rho}(1-v)|\nabla u|, \tag{1.12}$$

with the boundary and initial conditions

$$\left.\frac{\partial u}{\partial n}\right|_{\partial\Omega\times R_+} = 0, \qquad \left.\frac{\partial v}{\partial n}\right|_{\partial\Omega\times R_+} = 0, \tag{1.13}$$

$$u(x,0) = I(x), \qquad v(x,0) = \frac{2\alpha\rho|\nabla u|}{1+2\alpha\rho|\nabla u|}. \tag{1.14}$$

We can see that equation (1.11) is the evolution of the elliptic equation obtained from the Euler-Lagrange equation of $E(u,v)$ (the first variation with respect to u) by multiplying $|\nabla u|/\alpha(1-v)$ rather than the flow of the actual Euler-Lagrange equation. Compared with the evolution of the actual Euler-Lagrange equation, equation (1.11) has some good properties. First, the diffusion term $(1-v)|\nabla u| \operatorname{div}(\nabla u/|\nabla u|)$ has the same geometric interpretation as the diffusion term in (1.9). Second, the term $\nabla v \cdot \nabla u/|\nabla u|$ in the flow of the actual Euler-Lagrange equation is replaced by $\nabla v \cdot \nabla u$ in (1.11), this reduces the error in the numerical implementation. Moreover, due to the presence of the term $\nabla v \cdot \nabla u$, equation (1.11) is parabolic only along the level curves of u and it is hyperbolic in the direction normal to the level curves. This allows the solution u to develop shocks on the edges.

From the models mentioned above, we can see that heat equations with different structures are often used to solve the same minimization problem. In this note, we shall propose a new diffusion equation, which consists of (1.7′) with $\alpha(x)$ as in (1.8) and with the initial and boundary conditions (1.2),(1.3). In the next section, we will describe this model more precisely. In the third section, we shall state the theorem for the existence, uniqueness, and stability of our proposed model. The theorem can be proved by a similar argument developed in [6], but due to the presence of two extra nonlinear terms, more careful estimates are needed. We shall give a modified proof in the Appendix. In the fourth section, we will give the numerical results which indicate the new model is able to preserve edges and corners better than the existing methods.

2. DESCRIPTION OF THE PROPOSED MODEL

In this note, we propose the following model:

$$u_t = g^2|\nabla u| \operatorname{div}\left(\frac{\nabla u}{|\nabla u|}\right) + g\nabla g \cdot \nabla u - \beta g|\nabla u|(u-I), \qquad x\in\Omega, \quad t>0, \tag{2.1}$$

$$u(x,0) = I(x), \qquad x\in\Omega, \tag{2.2}$$

$$\left.\frac{\partial u}{\partial n}\right|_{\partial\Omega\times R_+} = 0, \qquad x\in\partial\Omega, \quad t>0, \tag{2.3}$$

where $g = g(\nabla G_\sigma * u)$ is determined in (1.8) and $\beta > 0$ is a parameter.

Note that the diffusion term in equation (1.6) with $\alpha(x)$ determined in (1.8) is given by

$$g\,(\nabla G_\sigma * u) \operatorname{div}\left(\frac{\nabla u}{|\nabla u|}\right). \tag{2.4}$$

As mentioned in the first section, the diffusion term in (1.9) is the product of (2.4) and $|\nabla u|$, while the diffusion term in (2.1) is the product of (2.4) and $g(\nabla G_\sigma * u)|\nabla u|$. The term $|\nabla u|$ has larger

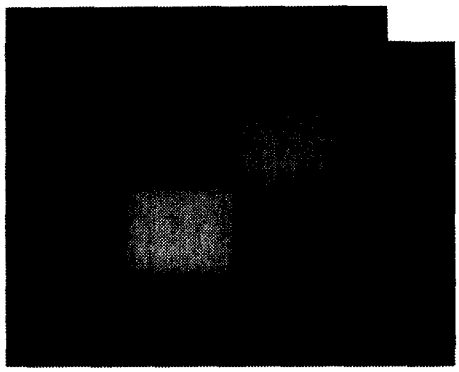

(a) Noiseless image.

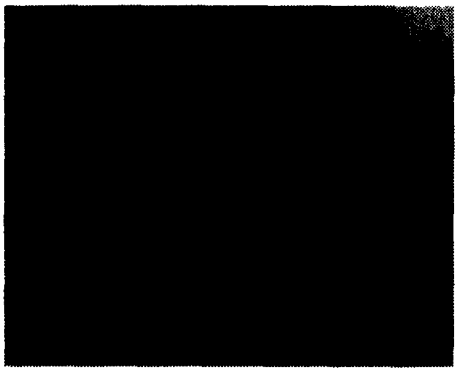

(b) Noisy version (SNR = 0 db).

(c) Reconstructed image by proposed model.

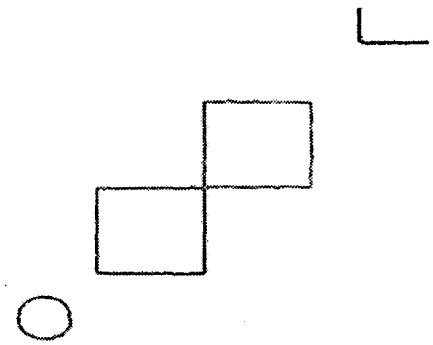

(d) Segmentation of the reconstructed image (c).

(e) The reconstructed image obtained by (1.9).

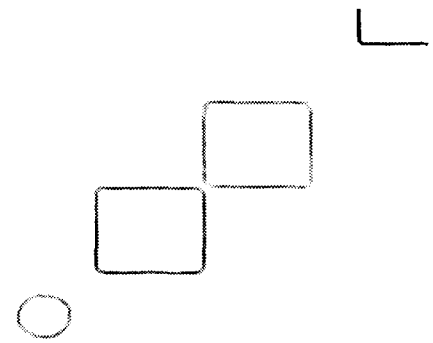

(f) The segmentation of image (e).

Figure 1.

value on the edges than in the homogeneous region, while $g(\nabla G_\sigma * u)|\nabla u| = |\nabla u|/(1+K|\nabla G_\sigma * u|^2)$ is just the opposite. Therefore, the diffusion applied by (1.9) may cause over smoothing near the edges, while this problem can be solved by using the proposed model (2.1). Figures 1e, 2e, and 6e show the reconstructed images by using model (1.9). One can see that in order to clean up the background, some of the edges, in particular, the corners are lost and the originally connected squares and triangles are becoming separated. To solve this problem, that means to regularize the homogeneous region with the least smoothing on the edges, we propose to use (2.1). Equation (2.1) not only keeps the good features that (1.9) has (as mentioned in Section 1), but also performs less smoothing on the edges compared with (1.9). The numerical results indicate that when the number of iterations reaches certain levels, then there is very little effect to the edges by running more iterations to smooth the homogeneous regions. We can see that the reconstructed image in Figures 1c, 2f, and 6c are better than that in Figures 1e, 2e, and 6e, respectively. For

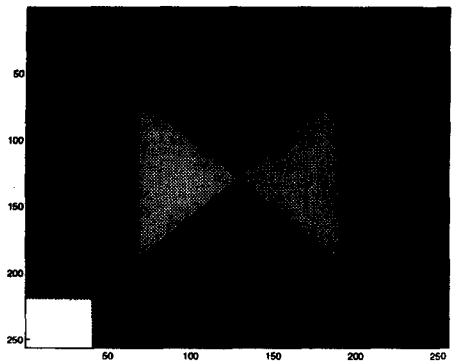

(a) Noiseless image.

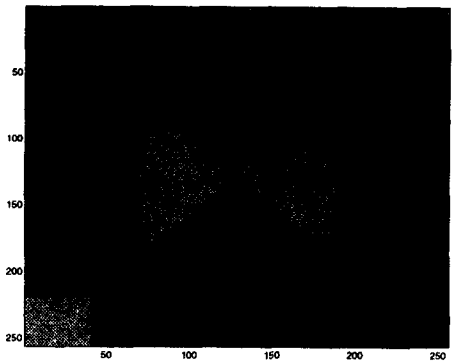

(b) Noisy version (SNR = 0 db).

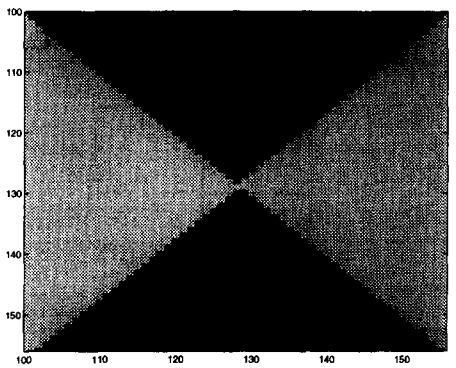

(c) Noiseless detail d.

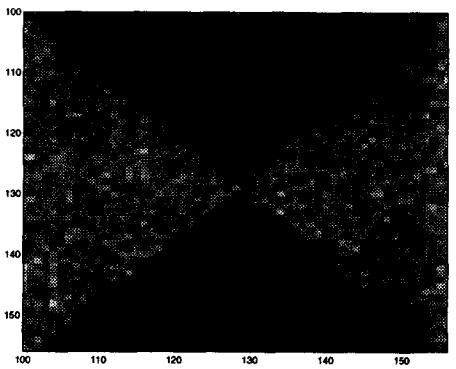

(d) Noisy detail d.

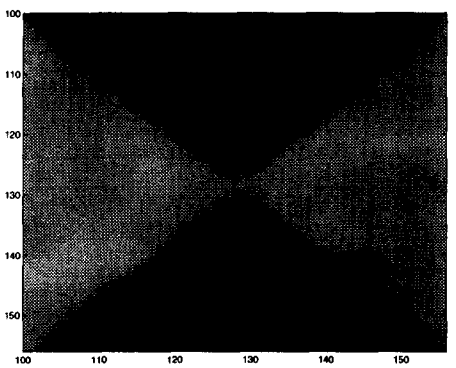

(e) Detail d of the reconstructed image by (1.9).

(f) Detail d of the reconstructed image by proposed model.

Figure 2.

instance, in Figure 1c, the homogeneous regions of the image are more smoothed, the boundaries of the squares are better preserved, and the squares are still linked.

3. EXISTENCE, UNIQUENESS, AND STABILITY

Since equation (2.1) is highly nonlinear and degenerate, we need the notion of so-called viscosity solution (see [8]). In this section, we will prove the existence, uniqueness, and stability for the viscosity solution to equation (2.1).

Our model equation is in two dimensions, mathematically we can study this problem for n-dimensional cases. σ, β, and K are constants in (2.1), and they do not affect the proof of well-posedness. To simplify the presentation, we shall consider $\sigma = \beta = K = 1$ and work with periodic boundary conditions. Then, by periodic extension, we consider the following Cauchy

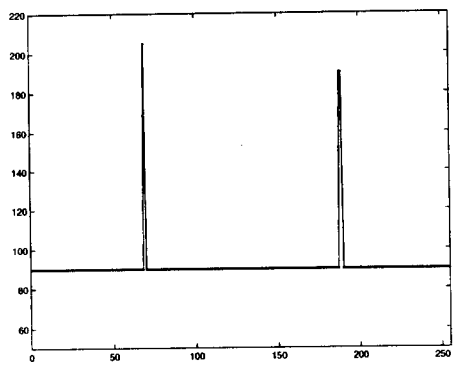

(a) Noiseless image.

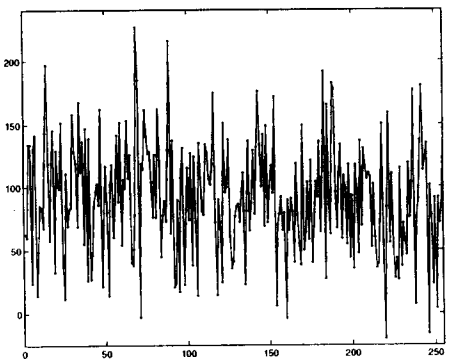

(b) Noisy image.

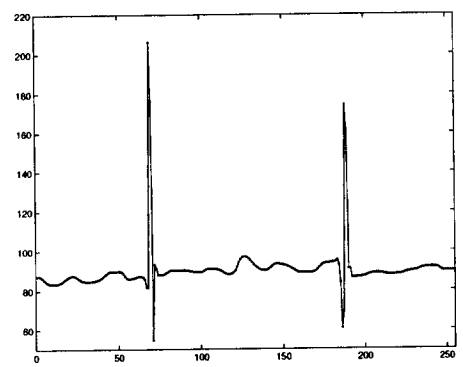

(c) Reconstructed image obtained by (2.1).

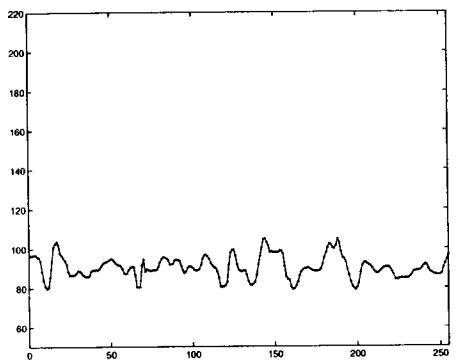

(d) Reconstructed image obtained by (1.9).

Figure 3. Plots of the lines $y = 188$.

problem:

$$\begin{aligned} \frac{\partial u}{\partial t} &= g^2 a_{ij}(\nabla u) u_{x_i x_j} + g\frac{\partial g}{\partial l}\left[(\nabla G_{x_l} * u)\cdot \nabla u\right] - g|\nabla u|(u - I), \qquad x \in R^n, \quad t \in R_+, \\ u(x,0) &= I(x), \qquad x \in R^n, \end{aligned} \tag{3.1}$$

where $g = g(s) = 1/(1+|s|^2)$, $s = (s_1, \ldots, s_n) = \nabla G * u$, $\frac{\partial g}{\partial l} = \frac{\partial g}{\partial s_l}(s)$, $G = (1/4\pi)\exp\{-(x^2 + y^2)/4\}$, $a_{ij}(p) = \delta_{ij} - p_i p_j/|p|^2$, and the summation convention is used.

First, let us recall the definition of viscosity subsolution of (3.1). A function $u \in C(R^n \times [0,T])$ for some $T > 0$ is said to be a viscosity subsolution of (3.1), if for all $\phi \in C^2(R^2 \times R)$, the following condition holds at any point $(x_0, t_0) \in R^n \times (0,T]$, at which $(u - \phi)$ attains a local maximum:

$$\begin{aligned} &\frac{\partial \phi}{\partial t}(x_0,t_0) - g\left((\nabla G * u)(x_0,t_0)\right)^2 a_{ij}\left(\nabla\phi(x_0,t_0)\right)\phi_{x_i x_j}(x_0,t_0) \\ &+g\left((\nabla G * u)(x_0,t_0)\right)\frac{\partial g}{\partial l}\left((\nabla G * u)(x_0,t_0)\right)\left[(\nabla G_{x_l} * u)(x_0,t_0)\cdot\nabla\phi(x_0,t_0)\right] \\ &-g\left((\nabla G * u)(x_0,t_0)\right)|\nabla\phi(x_0,t_0)|\left(u - I\right)(x_0,t_0)] \le 0, \qquad \text{if } \nabla\phi(x_0,t_0) \neq 0, \end{aligned} \tag{3.2}$$

$$\frac{\partial \phi}{\partial t}(x_0,t_0) - \left(g\left((\nabla G * u)(x_0,t_0)\right)\right)^2 \limsup_{p\to 0} a_{ij}(p)\phi_{x_i x_j}(x_0,t_0) \le 0, \qquad \text{if } \nabla\phi(x_0,t_0) = 0. \tag{3.3}$$

A viscosity supersolution is similarly defined by substituting "local maximum" for "local minimum", "≤ 0" for "≥ 0", and "limsup" for "liminf" in equations (3.2) and (3.3), respectively. A viscosity solution is a continuous function which is both a subsolution and a supersolution. We now state the theorem.

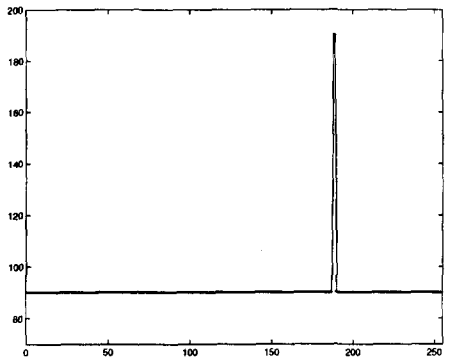

(a) Noiseless image.

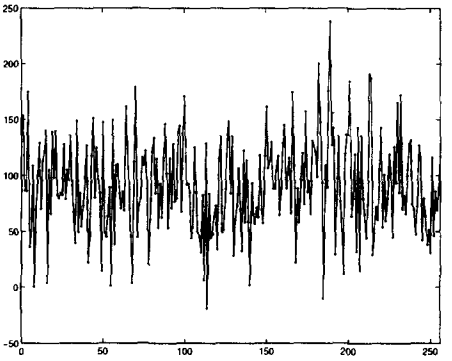

(b) Noisy image.

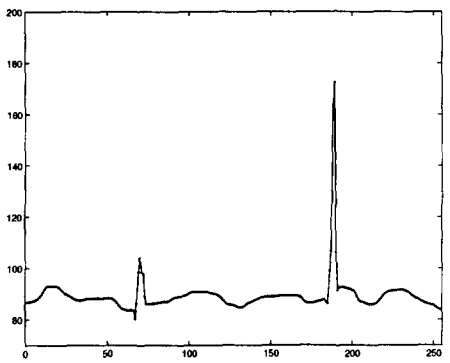

(c) Reconstructed image obtained by (2.1).

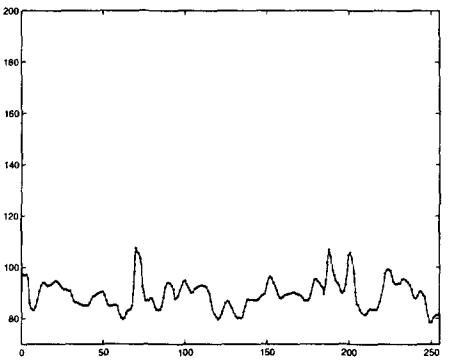

(d) Reconstructed image obtained by (1.9).

Figure 4. Plots of the lines $y = 69$.

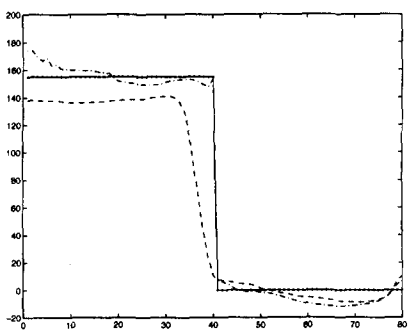

(a) Noiseless image (-), model (1.9) (--), proposed model $(\cdot - \cdot)$.

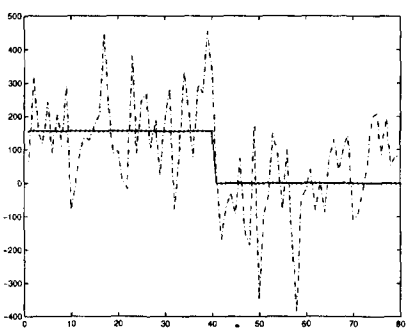

(b) Noiseless image (-) and noisy image $(\cdot - \cdot)$.

Figure 5. Cross-section for the lines $y = 220$.

THEOREM 3.1. *The Cauchy problem (3.1) has a unique viscosity solution* $u \in C(R^n \times [0,T]) \cap L^\infty(0,T;W^{1,\infty}(R^n))$ *for any* $T \in [0,\infty)$, *and* $\inf_{R^n} I \leq u(x,t) \leq \sup_{R^n} I$, *provided that* I *is Lipschitz continuous in* R^n.

Moreover, if $v \in C(R^n \times R_+)$ *is a viscosity solution of (3.1) with* I *replaced by a Lipschitz continuous function* I_1, *then for all* $T \in [0,+\infty)$, *there exists a constant* $C > 0$, *depending only on* I, I_1, *and* T, *such that*

$$\sup_{0\leq t\leq T} \|u(x,t) - v(x,t)\|_{L^\infty(R^n)} \leq C\|I - I_1\|_{L^\infty(R^n)}.$$

The proof of this theorem follows the argument developed in [6] for equation (1.9′). However, since our model has two more nonlinear terms than model (1.9′), more careful estimates are required, especially in getting the uniform L^∞-norm estimate for the gradient of the approximate

(a) Noiseless image.

(b) Noisy version (SNR = −6.02 db).

(c) Reconstructed image obtained by (2.1).

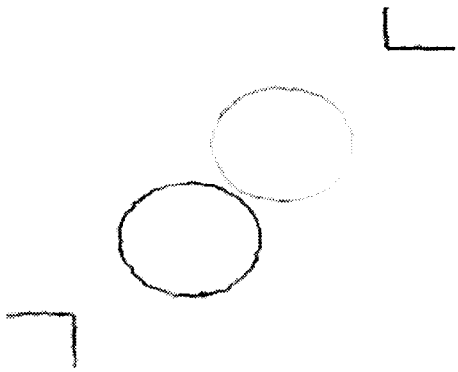

(d) Segmentation of image in (c).

(e) The reconstructed image obtained by (1.9).

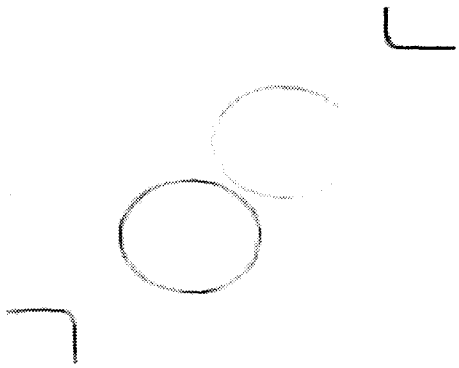

(f) The segmentation of image (e).

Figure 6.

solutions and in establishing the estimate $\sup_{\Omega\times[0,T]}|u-v| \le C\sup_{\Omega\times\{t=0\}}|u-v|$, where u and v are two viscosity solutions of (3.1). For the convenience of the reader, we shall give the proof in the Appendix.

4. NUMERICAL IMPLEMENTATION AND EXPERIMENTAL RESULTS

In this section, we present the results of applying the model in (1.9) and the proposed model in (2.1) on three images of varying difficulty. Numerical solutions of equations (1.9) and (2.1) are obtained by applying appropriate finite-difference methods as developed in [1,7,9,11], which are briefly described below.

Our images are represented by 256 × 256 matrices of intensity values. We let u_{ij} denote the value of the intensity of the image u at the pixel $(x = i\Delta t,\ y = j\Delta t)$. We denote $u(i, j, t_n)$ by $u^n_{i,j}$.

The time derivative u_t at (i, j, t_n) is approximated by the forward difference $(u_{i,j}^{n+1} - u_{i,j}^n)/\Delta t$. The diffusion term

$$|\nabla u| \left(\operatorname{div} \left(\frac{\nabla u}{|\nabla u|} \right) \right) = \frac{u_x^2 u_{yy} - 2u_x u_y u_{xy} + u_y^2 u_{xx}}{u_x^2 + u_y^2}$$

in (1.9) and (2.1) is approximated using central differences.

The term $\nabla g \cdot \nabla u$ permits the development of discontinuities which indicate the presence of object boundaries. Here, the main idea is to use forward or backward finite differences in computing the spatial derivatives of u in a manner that is consistent with the development of the shock, and it does not reflect the smoothness that may occur near the shock region. This feature is achieved by the following scheme developed by Osher and Sethian [9] (also used in [7]). Let

$$\begin{aligned} \Delta_x^+ u_{i,j} &= u_{i+1,j} - u_{i,j}, & \Delta_x^- u_{i,j} &= u_{i,j} - u_{i-1,j}, \\ \Delta_y^+ u_{i,j} &= u_{i,j+1} - u_{i,j}, & \Delta_y^- u_{i,j} &= u_{i,j} - u_{i,j-1}, \\ \Delta_x u_{i,j} &= \frac{u_{i+1,j} - u_{i-1,j}}{2}, & \Delta_y u_{i,j} &= \frac{u_{i,j+1} - u_{i,j-1}}{2}. \end{aligned}$$

Then we have

$$\begin{aligned} (\nabla g \cdot \nabla u)_{i,j} = {} & \max(\Delta_x g_{i,j}, 0)\, \Delta_x^- u_{i,j} + \min(\Delta_x g_{i,j}, 0)\, \Delta_x^+ u_{i,j} \\ & + \max(\Delta_y g_{i,j}, 0)\, \Delta_y^- u_{i,j} + \min(\Delta_y g_{i,j}, 0)\, \Delta_y^+ u_{i,j}. \end{aligned}$$

A complete discussion on this scheme is found in [9,10].

Using Neumann boundary conditions, we compute u_{ij}^{n+1}, $n = 1, 2, \ldots, N$, by

$$u_{ij}^{n+1} = u_{ij}^n + \Delta t \mathcal{L}\left(u_{ij}^n\right),$$

with $u_{ij}^0 = I(x_i, y_i)$ and

$$\mathcal{L}(u) = g^2 |\nabla u| \operatorname{div} \left(\frac{\nabla u}{|\nabla u|} \right) + g \nabla g \cdot \nabla u - \beta g |\nabla u| (u - I).$$

The following results are presented for two-dimensional images. We chose the parameters which give the best result in these models. We considered an image to be a "good" enhancement if the background was reasonably clear of structures attributable to noise, and if the edges were clearly defined. Our test images were of size 256×256 pixels. The noiseless images were gray-level piecewise-constant objects. The noise version I was obtained from the noiseless synthetic image by adding Gaussian noise with zero mean. Although the noiseless image only contains intensities between 0 and 255, the addition of noise results in pixel values which are outside of this range. In this paper, we do not truncate the noisy pixel values, so our noisy images contain intensities well outside the 0–255 range. For instance, the noisy image in Figure 5 contains intensities as low as -530 and as high as 641. This presents a greater challenge to algorithms than the truncated versions. We use Matlab to display the images.

Our first example is an image containing one circle and three squares. It is a grey-scale image with standard deviation equaling 38.1 and mean equaling 112.5 . Figure 1a presents the synthetic original noiseless image, and Figure 1b shows the noisy version. The signal-to-noise ratio (i.e., the ratio between the standard deviation of noise-free image and the standard deviation of the noise) is 0.0 db. The discretization of the model equation (1.9) was run with $\beta = 0.005$, $K = 0.0001$ for 200 iterations and produced the segmentation in Figure 1f (right) and the denoised image in Figure 1e (left). The proposed model (2.1) was run for 150 iterations with $\beta = 0.1$, $K = 0.0003$.

This produced the segmentation in Figure 1d (right) and the denoised image in Figure 1c (left). We get $\sigma = 0.5$ for each model.

Similar tests for the original image in Figure 2 were performed. The SNR is also 0.0 db and the standard deviation of the noiseless image is 42.7 and the mean is 104.5. Figures 2a and 2b show the original noiseless image and its noisy version, respectively. In the second test, we use the same parameters as in our first test.

To better illustrate the reconstruction, we presented in Figures 2c–f only the images on the subregion $d = \{(x, y) \in \Omega, \text{ s.t. } x \in [100, 156] \text{ and } y \in [100, 156]\}$. Figures 2c and 2d show the noiseless image and its noisy version detailed on d. In Figure 2e, we show the detail of the reconstructed image on d obtained by using model (1.9) after 150 iterations. Figure 2f shows the reconstructed image on d obtained by applying the proposed model after 150 iterations. We also present in Figure 3 and Figure 4 the profiles on lines for the images corresponding to Figure 2. In Figure 3, we use the 188^{th} row. In the original image, this row contains two single pixels of high intensity which sit at the bottom of the triangles. In Figure 4, we use the 69^{th} row. In the original image, this row contains a single pixel of high intensity which sits on the top of the triangle on the right side of the image. These plots illustrate that model (1.9) is unable to resolve small detail, which is clearly resolved by the proposed model. We can see that the edges are better preserved by using the proposed model, while the jumps have been completely lost by using (1.9).

In the last experiment, an application of our model in denoising and segmentation of the noisy image is presented in Figure 6b. Here the SNR is -6.0 db. The noiseless image containing two circles and two squares has standard deviation 63.3; mean is 29.8. The discretization of model equation (1.9) was run with $\beta = 0.0005$, $K = 0.00005$, $\Delta t = 0.1$ for 300 iterations, and it produced the segmentation in Figure 6f (right) and the denoised image in Figure 6e (left). The proposed model was run for 150 iterations with $\beta = 0.1$, $K = 0.00002$, and $\Delta t = 0.2$. This produced the segmentation in Figure 6d (right) and the denoised image in Figure 6c (left). In order to see the improvement of the proposed model clearly, line plots of the images are presented in Figure 5. Here, we use the 220^{th} row from column 1 to 80. These illustrate that the edges have been over smoothed using model (1.9), while the location of the edges are better preserved with the proposed model.

APPENDIX

PROOF OF THEOREM 3.1. We shall outline the proof in several stages.

STEP 1. We first show that if u is a viscosity solution of (3.1) on $R^n \times R_+$, then

$$\inf_{R^n} I \leq u \leq \sup_{R^n} I, \qquad \text{on } R^n \times [0, \infty). \tag{5.1}$$

Let $\phi = \sup_{R^n} I + \delta t$ (where $\delta > 0$) in (3.2) and assume that $u - \phi$ attains a local maximum at (x_0, t_0) with $t_0 > 0$, then $\nabla\phi(x_0, t_0) = 0$, and from equation (3.2), $\frac{\partial \phi}{\partial t}(x_0, t_0) \leq 0$. This contradicts $\frac{\partial \phi}{\partial t} \equiv \delta > 0$ on $R^n \times [0, \infty)$. Therefore, $u - \phi$ must attain its maximum at $t_0 = 0$. So,

$$u - \phi \leq \sup \left(I - \sup_{R^n} I \right),$$
$$u \leq \sup_{R^n} I + \delta t.$$

Similarly, we have (from the definition of supersolution)

$$u \geq \inf_{R^n} I - \delta t.$$

Letting $\delta \to 0$ proves (5.1).

STEP 2. Next we prove the gradient estimate for the approximate solution. Consider the following Cauchy problem:

$$\begin{aligned} \frac{\partial u^\varepsilon}{\partial t} &= (g^\varepsilon)^2 a_{ij}^\varepsilon (\nabla u^\varepsilon) u_{x_i x_j}^\varepsilon + g^\varepsilon \frac{\partial g^\varepsilon}{\partial l} (\nabla G_{x_l} * u^\varepsilon) \cdot \nabla u^\varepsilon - b^\varepsilon (\nabla u^\varepsilon) g^\varepsilon (u^\varepsilon - I^\varepsilon), \\ & x \in R^n, \quad t \in R_+, \\ u^\varepsilon(x,0) &= I^\varepsilon(x), \qquad x \in R^n, \end{aligned} \tag{5.2}$$

where

$$\begin{aligned} & 0 < \varepsilon < 1, \\ g^\varepsilon &= g(\nabla G * u^\varepsilon) + \varepsilon, \\ a_{ij}^\varepsilon(p) &= (\varepsilon + 1)\delta_{ij} - \frac{P_i P_j}{|P|^2 + \varepsilon^2}, \\ b^\varepsilon(p) &= \sqrt{|p|^2 + \varepsilon}, \end{aligned}$$

$I^\varepsilon \in C^\infty(R^n)$ (periodic) such that $I^\varepsilon \to I$ uniformly and
$\|\nabla I^\varepsilon\|_{L^\infty(R^n)} \le \|\nabla I\|_{L^\infty(R^n)}$, $\|I^\varepsilon\|_{L^\infty(R^n)} \le \|I\|_{L^\infty(R^n)}$.

By the theory of quasi-linear uniformly parabolic equations [11, Section 6, Theorem 4.4], problem (5.2) admits a smooth solution $u^\varepsilon \in C^\infty(R^n \times R_+)$. Since any smooth solution is a viscosity solution, by an argument similar to that in Step 1, we know that

$$|u^\varepsilon| \le M, \qquad \text{for } (x,t) \in R^n \times [0,\infty), \tag{5.3}$$

where $M > 0$ is a constant depending only on I. Now we shall show a uniform estimate for $|\nabla u^\varepsilon|_{L^\infty(R^n)}$.

Differentiating (5.2) with respect to x_k, then multiplying the resulting equation by $2u_{x_k}^\varepsilon$, and taking a summation with respect to k, we get

$$\begin{aligned} & \frac{\partial |\nabla u^\varepsilon|^2}{\partial t} - (g^\varepsilon)^2 a_{ij}^\varepsilon \frac{\partial^2 |\nabla u^\varepsilon|^2}{\partial x_i \partial x_j} - (g^\varepsilon)^2 \frac{\partial a_{ij}^\varepsilon}{\partial l} u_{x_i x_j}^\varepsilon \frac{\partial |\nabla u^\varepsilon|^2}{\partial x_l} \\ & - g^\varepsilon \frac{\partial g^\varepsilon}{\partial l} \left[(\nabla G_{x_l} * u^\varepsilon) \cdot \left(\nabla |\nabla u^\varepsilon|^2 \right) \right] + g^\varepsilon \frac{\partial b^\varepsilon}{\partial m} (u^\varepsilon - I^\varepsilon) \frac{\partial |\nabla u^\varepsilon|^2}{\partial x_m} \\ & = 4 g^\varepsilon \frac{\partial g^\varepsilon}{\partial l} (G_{x_l x_k} * u^\varepsilon) a_{ij}^\varepsilon u_{x_i x_j}^\varepsilon u_{x_k}^\varepsilon - 2 (g^\varepsilon)^2 a_{ij}^\varepsilon u_{x_k x_i}^\varepsilon u_{x_k x_i}^\varepsilon u_{x_k x_j}^\varepsilon + F \\ & =: I + II + III, \end{aligned} \tag{5.4}$$

where

$$\begin{aligned} F = & 2 \left(g^\varepsilon \frac{\partial^2 g^\varepsilon}{\partial l \partial m} + \frac{\partial g^\varepsilon}{\partial m} \frac{\partial g^\varepsilon}{\partial l} \right) (G_{x_m x_k} * u^\varepsilon) \left[(\nabla G_{x_l} * u^\varepsilon) \cdot \nabla u^\varepsilon \right] u_{x_k}^\varepsilon \\ & + 2 g^\varepsilon \frac{\partial g^\varepsilon}{\partial l} \left[(\nabla G_{x_l x_k} * u^\varepsilon) \cdot \nabla u^\varepsilon \right] u_{x_k}^\varepsilon \\ & - 2 b^\varepsilon \left(u_{x_k}^\varepsilon - I_{x_k}^\varepsilon \right) u_{x_k}^\varepsilon \left[g^\varepsilon - \frac{\partial g^\varepsilon}{\partial m} (G_{x_m x_k} * u^\varepsilon) g^\varepsilon \right], \\ g^\varepsilon = g^\varepsilon(\nabla G * u^\varepsilon), \qquad & a_{ij}^\varepsilon = a_{ij}^\varepsilon(\nabla u^\varepsilon), \qquad b^\varepsilon = b^\varepsilon(\nabla u^\varepsilon), \end{aligned} \tag{5.5}$$

and $\frac{\partial g^\varepsilon}{\partial l}$ stands for the partial derivative of g^ε with respect to its l^{th} component evaluated at $\nabla G * u^\varepsilon$. From the definitions of a_{ij}^ε, b^ε, and g^ε, we can verify that

$$\begin{aligned} & 2 a_{ij}^\varepsilon u_{x_k x_j}^\varepsilon \ge \left| a_{ij}^\varepsilon u_{x_i x_j}^\varepsilon \right|^2, \\ & \left| g^\varepsilon \frac{\partial g^\varepsilon}{\partial l} \right| \le 2 (g^\varepsilon)^2, \end{aligned}$$

and for any multi-index α with $|\alpha| \leq 2$,

$$\begin{aligned} \left|D_p^\alpha b^\varepsilon(p)\right| &\leq C, \qquad \forall\, p \in R^n, \\ \left|D_s^\alpha g(s)\right| &\leq C, \qquad \forall\, s \in R^n, \\ \left|D_x^\alpha G * u\right| &\leq C, \qquad \forall\, x \in R^n. \end{aligned} \tag{5.6}$$

Combining (5.4)–(5.6) and using the Cauchy inequality, we have

$$I + II + III \leq C\left(|\nabla u^\varepsilon|^2\right), \tag{5.7}$$

where $C > 0$ is a constant depending only on M in (5.3), hence, C depends only on I. Applying the maximum principle [12] to (5.4) yields for all $t \in [0, T]$ (for any $T < \infty$),

$$\begin{aligned} \|\nabla u^\varepsilon(\cdot, t)\|_{L^\infty(R^n)} &\leq e^{ct} \|\nabla I^\varepsilon\|_{L^\infty(R^n)} \\ &\leq e^{ct} \|\nabla I\|_{L^\infty(R^n)} \leq C_T, \end{aligned} \tag{5.8}$$

where $C_T > 0$ depends only on T and I. This implies that

$$|u^\varepsilon(x,t) - u^\varepsilon(y,t)| \leq C_T |x - y|, \qquad \text{for } \forall\, x, y \in R^n \text{ and } \forall\, t \in [0,T].$$

By the same argument used in [6], we have

$$|u^\varepsilon(x,s) - u^\varepsilon(x,t)| \leq C_T |t - s|^{1/2}, \qquad \text{for } \forall\, x \in R^n \text{ and } \forall\, s, t \in [0,T].$$

Then, by the Ascoli-Arzela Theorem, there exists a subsequence u^{ε_k} of u^ε and a function $u \in C(R^n \times [0,T]) \cap L^\infty(0,T; W^{1,\infty}(R^n))$ such that as $\varepsilon_k \to 0$,

$$u^{\varepsilon_k} \to u, \qquad \text{locally uniformly in } R^n \times R_+. \tag{5.9}$$

STEP 3. Existence of viscosity solution. We assert now that u obtained in (5.9) is a viscosity solution of (3.1) in the sense of (3.2) and (3.3).

Let $\phi \in C^2(R^n \times R)$ and assume $u - \phi$ has a strict local maximum at a point $(x_0, t_0) \in R^n \times R_+$. As $u^{\varepsilon_k} \to u$ uniformly near (x_0, t_0), $u^{\varepsilon_k} - \phi$ has a local maximum at a point (x_k, t_k) with

$$(x_k, t_k) \to (x_0, t_0), \qquad \text{as } k \to \infty \tag{5.10}$$

and at (x_k, t_k),

$$\nabla u^{\varepsilon_k} = \nabla \phi, \quad u_t^{\varepsilon_k} = \phi_t, \qquad a_{ij}^{\varepsilon_k}(\nabla u^{\varepsilon_k})\, u_{x_i x_j}^{\varepsilon_k} \leq a_{ij}^{\varepsilon_k}(\nabla \phi)\, \phi_{x_i x_j}. \tag{5.11}$$

Therefore, (5.2) implies that at (x_k, t_k),

$$\frac{\partial \phi}{\partial t} - (g^{\varepsilon_k})^2 a_{ij}^{\varepsilon_k}(\nabla\phi)\phi_{x_i x_j} - g^{\varepsilon_k} \frac{\partial g^{\varepsilon_k}}{\partial l}[\nabla G_{x_l} * u^{\varepsilon_k} \cdot \nabla \phi] - b^{\varepsilon_k}(\nabla\phi) g^{\varepsilon_k}(u^{\varepsilon_k} - I^{\varepsilon_k})] \leq 0, \tag{5.12}$$

where $g^{\varepsilon_k} = g^{\varepsilon_k}(\nabla G * u^{\varepsilon_k})$, $\frac{\partial g^{\varepsilon_k}}{\partial l} = \frac{\partial g^{\varepsilon_k}}{\partial l}(\nabla G * u^{\varepsilon_k})$.

If $\nabla\phi(x_0, t_0) \neq 0$, from (5.10), for sufficiently large k, $\nabla\phi(x_k, t_k) \neq 0$. One may apply limits in (5.12) to obtain (recalling the definitions of a_{ij}^ε, g^ε, b^ε, and (5.9),(5.10)),

$$\frac{\partial \phi}{\partial t} - g^2 a_{ij}(\nabla\phi)\phi_{x_i x_j} - g \frac{\partial g}{\partial l}\left[(\nabla G_{x_l} * u) \cdot \nabla \phi\right] + b(\nabla\phi) g (u - I) \leq 0, \qquad \text{at } (x_0, t_0),$$

where $g = g(\nabla G * u)$, $\frac{\partial g}{\partial l} = \frac{\partial g}{\partial l}(\nabla G * u)$. This gives (3.2).

If $\nabla\phi(x_0,t_0)=0$, let

$$h^k=\frac{\nabla\phi\,(x_k,t_k)}{\sqrt{|\nabla\phi\,(x_k,t_k)|^2+\varepsilon^2}},$$

then (5.12) reduces to

$$\begin{aligned}\frac{\partial\phi}{\partial t}-(g^{\varepsilon_k})^2\left((\varepsilon_k+1)\,\delta_{ij}-h_i^kh_j^k\right)\phi_{x_ix_j}-g^{\varepsilon_k}\frac{\partial g^{\varepsilon_k}}{\partial l}\left[(\nabla G_{x_l}*u^{\varepsilon_k})\cdot\nabla\phi\right]\\ -b^{\varepsilon_k}(\nabla\phi)g^{\varepsilon_k}\,(u^{\varepsilon_k}-I^{\varepsilon_k})\le 0,\qquad \text{at } (x_k,t_k)\,.\end{aligned}\tag{5.13}$$

Since $\nabla\phi(x_k,t_k)\to 0$, $\varepsilon_k\to 0$ as $k\to\infty$, hence, $b^{\varepsilon_k}(\nabla\phi(x_k,t_k))\to 0$. Moreover, because $|h^k|\le 1$, there is a subsequence of h^k, also denoted by h^k, such that as $k\to\infty$, $h^k\to h$ in $R^n\times R$ with $|h|\le 1$. Applying limits to (5.13), we get

$$\frac{\partial\phi}{\partial t}-(g\,(\nabla G*u))^2\,(\delta_{ij}-h_ih_j)\,\phi_{x_ix_j}\le 0,\qquad \text{at } (x_0,t_0).\tag{5.14}$$

This is the same as (3.3). If $u-\phi$ has a local maximum, but not necessarily a strict local maximum at (x_0,t_0), we just need to repeat the argument above with $\phi(x,t)$ replaced by $\tilde\phi(x,t)=\phi(x,t)+|x-x_0|^4+(t-t_0)^4$. Therefore, u is a subsolution of (3.1). Similarly, we can show that u is a supersolution. Hence, u is a viscosity solution of (3.1).

STEP 4. UNIQUENESS. We will now prove the uniqueness and stability for the viscosity solution of (3.1). This proof is based on Theorem 8.3 in [8]. Let u be a viscosity solution of (3.1) with Lipschitz continuous initial data I and v be a viscosity solution of (3.1) with I replaced by a Lipschitz continuous function I_1. Let

$$\omega(x,y,t)=u(x,t)-v(y,t)-(4\delta)^{-1}|x-y|^4-\lambda t,\qquad t\in[0,T],\quad x,y\in R^n,$$

where $\delta>0$ and $\lambda>0$ are constants to be determined later.

CLAIM. $\omega(x,y,t)$ attains maximum at $t=0$ for an arbitrary positive constant λ.

Indeed, if $\omega(x,y,t)$ attains its maximum at some point (x_0,y_0,t_0) with $t_0>0$, by Theorem 8.3 in [8], for each $\mu>0$, there exist X and Y, $(n\times n)$-symmetric matrices, and $\alpha,\beta\in R$, such that

$$\alpha-\beta=\lambda,\tag{5.15}$$

$$\begin{pmatrix}X&0\\0&-Y\end{pmatrix}\le A+\mu A^2,\tag{5.16}$$

and

$$\begin{aligned}&\alpha-(g\,((\nabla G*u)\,(x_0,t_0)))^2\,a_{ij}\left(\delta^{-1}\,|x_0-y_0|^2\,(x_0-y_0)\right)X_{ij}\\ &\quad-g\,((\nabla G*u)\,(x_0,t_0))\,\frac{\partial g}{\partial l}\,((\nabla G*u)\,(x_0,t_0))\\ &\quad\times\left[(\nabla G_{x_l}*u)\,(x_0,t_0)\cdot\delta^{-1}\,|x_0-y_0|^2\,(x_0-y_0)\right]\\ &+\delta^{-1}\,|x_0-y_0|^3\,g\,((\nabla G*u))\,(x_0,t_0)\,(u\,(x_0,t_0)-I\,(x_0))\le 0,\end{aligned}\tag{5.17}$$

$$\begin{aligned}&\beta-(g\,((\nabla G*v)\,(y_0,t_0)))^2\,a_{ij}\left(\delta^{-1}\,|x_0-y_0|^2\,(x_0-y_0)\right)Y_{ij}\\ &\quad-g\,((\nabla G*v)\,(y_0,t_0))\,\frac{\partial g}{\partial l}\,((\nabla G*v)\,(y_0,t_0))\\ &\quad\times\left[(\nabla G_{x_l}*v)\,(y_0,t_0)\cdot\delta^{-1}\,|x_0-y_0|^2\,(x_0-y_0)\right]\\ &-\delta^{-1}\,|x_0-y_0|^3\,g\,((\nabla G*v)\,(y_0,t_0))\,(v\,(y_0,t_0)-I_1\,(y_0))\ge 0,\end{aligned}\tag{5.18}$$

where

$$A = (A_{ij})_{n\times n}, \qquad \text{and}$$
$$A_{ij} = \delta^{-1}|x_0 - y_0|^2\delta_{ij} + 2\delta^{-1}(x_0 - y_0)_i(x_0 - y_0)_j, \tag{5.19}$$

here $(x_0 - y_0)_i$ stands for the i^{th} component of $x_0 - y_0$.

We observe that $x_0 \neq y_0$. Indeed, if $x_0 = y_0$, then from (5.19), $A = 0$, hence, $X \leq 0$ and $Y \geq 0$ from (5.16). Thus, (5.17),(5.18) leads to $\alpha \leq 0$ and $\beta \geq 0$, which contradicts $\alpha - \beta = \lambda > 0$. We now choose

$$\mu = \delta\,|x_0 - y_0|^{-2}. \tag{5.20}$$

From (5.19) and (5.16) after some algebra, we have

$$\begin{pmatrix} X & 0 \\ 0 & -Y \end{pmatrix} \leq 2\delta^{-1}\begin{pmatrix} B & -B \\ -B & B \end{pmatrix}, \tag{5.21}$$

where

$$B_{ij} = |x_0 - y_0|^2\,\delta_{ij} + 5\,(x_0 - y_0)_i\,(x_0 - y_0)_j, \qquad 1 \leq i, \quad j \leq n.$$

Let

$$U = (\nabla G * u)\,(x_0, t_0), \qquad V = (\nabla G * v)\,(y_0, t_0),$$
$$D = a_{ij}\left(\delta^{-1}\,|x_0 - y_0|^2\,(x_0 - y_0)\right)_{1\leq i,\,j\leq n},$$

and

$$Q = \begin{pmatrix} g(U)^2D & g(U)g(V)D \\ g(U)g(V)D & g(V)^2D \end{pmatrix}.$$

Noting that Q is a nonnegative symmetric matrix, from (5.21), we have

$$Q\begin{pmatrix} X & 0 \\ 0 & -Y \end{pmatrix} \leq 2\delta^{-1}Q\begin{pmatrix} B & -B \\ -B & B \end{pmatrix}.$$

Taking the trace, we get

$$\begin{aligned} g(U)^2D_{ij}X_{ij} - g(V)^2D_{ij}Y_{ij} &\leq 2\delta^{-1}(g(U) - g(V))^2\,\mathrm{trace}(DB) \\ &\leq 4\delta^{-1}(g(U) - g(V))^2|x_0 - y_0|^2. \end{aligned} \tag{5.22}$$

Then, from (5.15), (5.17), and (5.18),

$$\lambda = \alpha - \beta \leq I + II + III, \tag{5.23}$$

where

$$I = g(U)^2D_{ij}X_{ij} - g(V)^2D_{ij}Y_{ij}, \tag{5.24}$$

$$\begin{aligned} II = \Big[&g(U)\frac{\partial g}{\partial l}(U)\,(\nabla G_{x_l} * u)\,(x_0, t_0) \\ &-g(V)\frac{\partial g}{\partial l}(V)\,(\nabla G_{x_l} * v)\,(y_0, t_0)\Big] \cdot \delta^{-1}\,|x_0 - y_0|^2\,(x_0 - y_0), \end{aligned} \tag{5.25}$$

$$\begin{aligned} III = {} & g^2(U)\delta^{-1}\,|x_0 - y_0|^3\,(u\,(x_0, t_0) - I\,(x_0, t_0)) \\ & - g^2(V)\delta^{-1}\,|x_0 - y_0|^3\,(v\,(x_0, t_0) - I_1\,(y_0)). \end{aligned} \tag{5.26}$$

We now estimate (5.24)–(5.26). First,

$$\begin{aligned} &|U - V| \leq |(\nabla G * u)\,(x_0, t_0) - (\nabla G * v)\,(x_0, t_0)| \\ &+ |(\nabla G * v)\,(x_0, t_0) - (\nabla G * v)\,(y_0, t_0)| \leq C\left(\sup_{R^n\times[0,T]}|u - v| + |x_0 - y_0|\right). \end{aligned} \tag{5.27}$$

Then, by the mean value theorem,

$$|g(U) - g(V)| \leq C|U - V|, \tag{5.28}$$

$$\begin{aligned} &\left|g(U)\frac{\partial g}{\partial l}(U)\left(\nabla G_{x_l} * u\right)(x_0,t_0) - g(V)\frac{\partial g}{\partial l}(V)\left(\nabla G_{x_l} * v\right)(y_0,t_0)\right| \\ &\leq \left|g(U)\frac{\partial g}{\partial l}(U) - g(V)\frac{\partial g}{\partial l}(V)\right| \left|\left(\nabla G_{x_l} * u\right)(x_0,t_0)\right| \\ &+ \left|g(V)\frac{\partial g}{\partial l}(V)\right| \left|\left(\nabla G_{x_l} * u\right)(x_0,t_0) - \left(\nabla G_{x_l} * v\right)(y_0,t_0)\right| \leq C|U - V|, \end{aligned} \tag{5.29}$$

$$\begin{aligned} &\left|g^2(U)u(x_0,t_0) - g^2(V)v(y_0,t_0)\right| \\ &\leq \left|g^2(U) - g^2(V)\right| \left|u(x_0,t_0)\right| + \left|g^2(V)\right| \left|u(x_0,t_0) - v(y_0,t_0)\right| \\ &\leq C\left(|U - V| + |u(x_0,t_0) - v(y_0,t_0)|\right). \end{aligned} \tag{5.30}$$

Similarly,

$$\left|g^2(V)I(x_0,t_0) - g^2(V)I_1(y_0,t_0)\right| \leq C\left(|U - V| + |I(x_0,t_0) - I_1(x_0,t_0)|\right). \tag{5.31}$$

The constants $C > 0$ in (5.28)–(5.31) depend only on I, I_1, and the Lipschitz constants for u and v. By using estimates (5.27)–(5.31) and definitions (5.23)–(5.26), we get

$$\lambda \leq C\delta^{-1}\left[\left(\sup_{R^n\times[0,T]}|u - v|\right)^2 |x_0 - y_0|^2 + |x_0 - y_0|^4 + \left(\sup_{R^n\times[0,T]}|u - v|\right)|x_0 - y_0|^3\right]. \tag{5.32}$$

On the other hand, since (x_0, y_0, t_0) is the maximum point of $\omega(x, y, t)$,

$$u(x_0,t_0) - v(x_0,t_0) - (4\delta)^{-1}|x_0 - y_0|^4 - \lambda t_0 \geq u(y_0,t_0) - v(y_0,t_0) - \lambda t_0.$$

This leads to

$$|x_0 - y_0| \leq (4\delta L)^{1/3}, \tag{5.33}$$

where L is a Lipschitz constant for u in $R^n \times [0,T]$. Combining this with (5.32) yields

$$\begin{aligned} \lambda &\leq C\delta^{-1}\left\{\left(\sup_{R^n\times[0,T]}|u - v|\right)^2 (4\delta L)^{2/3} + \left(\sup_{R^n\times[0,T]}|u - v|\right)4\delta L + (4\delta L)^{4/3}\right\} \\ &\leq C_0\left\{\delta^{-1/3}\left(\sup_{R^n\times[0,T]}|u - v|\right)^2 + \sup_{R^n\times[0,T]}|u - v| + \delta^{1/3}\right\}, \end{aligned} \tag{5.34}$$

where $C_0 > 0$ depends only on I, I_1, and the Lipschitz constants of u and v. We now set

$$\delta = L^{-4}\left(\sup_{R^n\times[0,T]}|u - v|\right)^3 \tag{5.35}$$

and from (5.34), we obtain

$$\lambda \leq C_0\left(L^{4/3} + L^{-4/3} + 1\right)\sup_{R^n\times[0,T]}|u - v|. \tag{5.36}$$

Let

$$\lambda = C_0\left(L^{4/3} + L^{-4/3} + 2\right)\sup|u - v|. \tag{5.37}$$

This leads to a contradiction with (5.36). Therefore, for the choice (5.37) of λ, $\omega(x,y,t)$ attains its maximum at $t=0$, which is our claim. Hence,

$$\begin{aligned} u(x,t)-v(y,t)-(4\delta)^{-1}|x-y|^4-\lambda t &\\ \leq \sup_{x,y\in R^n}&\left(u(x,0)-v(y,0)-(4\delta)^{-1}|x-y|^4\right)\\ \leq \sup_{x,y\in R^n}&\left(I(y)-I_1(y)+I(x)-I(y)-(4\delta)^{-1}|x-y|^4\right)\\ \leq \sup_{R^n}&|I-I_1|+\sup_{|x-y|\geq 0}\left(I(x)-I(y)-(4\delta)^{-1}|x-y|^4\right)\\ \leq \sup_{R^n}&|I-I_1|+\sup_{|x-y|\geq 0}\left(L|x-y|-(4\delta)^{-1}|x-y|^4\right). \end{aligned} \tag{5.38}$$

Noticing that $\sup_{r\geq 0}(Lr-(4\delta)^{-1}r^4)$ is achieved at $r=(\delta L)^{1/3}$, and letting $x=y$ in (5.38), from (5.35) and (5.37), we get

$$\sup_{R^n\times[0,T]}|u-v|\leq \sup_{R^n}|I-I_1|+\frac{3}{4}\sup_{R^n\times[0,T]}|u-v|+C_0\left(L^{4/3}+L^{-4/3}+2\right)T\sup_{R^n\times[0,T]}|u-v|. \tag{5.39}$$

Therefore, there exists $T_0>0$, sufficiently small ($T_0<1/(8C_0(L^{4/3}+L^{-4/3}+2))$) such that from (5.39), we have

$$\sup_{R^n\times[0,T_0]}|u-v|\leq 8\sup_{R^n}|I-I_1|. \tag{5.40}$$

For large t, by iteration, we easily obtain

$$\sup_{R^n\times[0,T]}|u-v|\leq C(T)\sup_{R^n}|I-I_1|.$$

This proves the uniqueness and stability for u.

REFERENCES

1. L. Rudin, S. Osher and E. Fatemi, Nonlinear total variation based noise removal algorithms, *Physica D* **60**, 259–268 (1992).
2. D. Strong and T. Chan, Spatially and scale adaptive total variation based regularization and anisotropic diffusion in image processing (preprint).
3. D.M. Strong, Adaptive total variation minimizing image restoration, Thesis, University of California (1997).
4. C.R. Vogel and M.E. Oman, Iterative methods for total variation denoising, *SIAM J. Sci. Statist. Comput.* **17**, 227–238 (1996).
5. Y. Chen, B.C. Vemuri and L. Wang, Image denoising and segmentation via nonlinear diffusion, *SIAM J. Appl. Math.* (submitted).
6. L. Alvarez, P.L. Lions and J.M. Morel, Image selective smoothing and edge detection by nonlinear diffusion, *SIAM J. Numer. Anal.* **29** (3), 845–866 (1992).
7. J. Shah, A common framework for curve evolution, segmentation and anisotropic diffusion, *IEEE Conf. on Computer Vision and Pattern Recognition* (June, 1996).
8. M.G. Crandall, H. Ishii and P.L. Lions, User's guide to viscosity solutions of second order partial differential equations, *Bulletin of the American Mathematical Society* **27** (1), 1–67 (1992).
9. S. Osher and J. Sethian, Fronts propagating with curvature dependent speed, Algorithms based on the Hamilton-Jacobi formulation, *J. Comp. Physics* **79**, 12–49 (1988).
10. R. Malladi, J. Sethian and B.C. Vemuri, A fast level set based algorithm for topology-independent shape modeling, *J. Mathematical Imaging and Vision* **6**, 269–289 (1996).
11. O.A. Ladyzhenskaya, V.A. Solonnikov and N.N. Uraltseva, *Linear and Quasilinear Equations of Parabolic Type*, American Mathematical Society, Providence, RI, (1968).
12. H. Brezis, *Analyse Fontionelle, Théorie et Applications*, Paris, (1987).